A kinematic dynamo model for accretion disks around Kerr black holes

Luca Del Zanna [1, 2, 3, *, @] , Niccolo' Bucciantini [2, 3, @] , Matteo Bugli [4, @]

1 : Dipartimento di Fisica e Astronomia, Universita' di Firenze

Via G. Sansone 1, Sesto Fiorentino - Italy

2 : INAF - Osservatorio Astrofisico di Arcetri

L.go Fermi 5 Firenze - Italy

3 : INFN - Sezione di Firenze

Via G. Sansone 1, Sesto Fiorentino - Italy

4 : MPA - Garching

Karl-Schwarzschild Strasse 1, Garching - Germany

* : Corresponding author

Ordered, large-scale magnetic fields are believed to be a fundamental ingredient in accretion processes that power the outflows and jets of AGNs and GRBs, especially in the Blandford-Znajek scenario where the central engine is a rotating black hole. However, the origin of such fields is still debated. A possibilty is a combination of the disk differential rotation and the likely presence of turbulence motions in the disk itself, which provides a mean-field alpha-Omega dynamo action, capable of enhancing any initial seed magnetic field. As a first astrophysical application of the ECHO code in its recent version supplemented by a generalized Ohm law, we present here a kinematic study of dynamo effects in thick accretion disks around Kerr black holes.

Subject :	:	oral
Topics	:	Plasmaphysics

A kinematic dynamo model for accretion disks around Kerr black holes

Luca Del Zanna

Dipartimento di Fisica e Astronomia, Università degli Studi di Firenze

INAF - Osservatorio Astrofisico di Arcetri

INFN - Sezione di Firenze

luca.delzanna@unifi.it

and: Matteo Bugli, Niccolò Bucciantini

Accretion and outflows throughout the scales, 2014, Lyon

Outline

1. Introduction to dynamo
   - Introduction
   - Mean-field dynamo in classical MHD
2. Non-ideal Ohm's law in $3+1$ GRMHD
   - The ECHO code for GRMHD
   - Covariant and $3+1$ formulations
   - IMEX schemes for stiff relaxation equations
   - Numerical tests
3. Kinematic dynamo in accretion tori
   - Initial equilibrium and set up
   - Study of the Ω effect vs resistivity
   - Study of the $\alpha-\Omega$ dynamo
4. Conclusions and future work
   - Conclusions
   - Future work

Introduction to dynamo

Amplification of Magnetic Fields

Ordered magnetic fields on large scales are a fundamental ingredient of processes related to accretion disks:

- magnetocentrifugally driven winds and jets (YSOs, AGNs),
- Blandford-Znajek mechanism from Kerr Black Holes (AGNs, collapsar model for GRBs).

A mean-field dynamo mechanism may do the job: *correlated* small-scale turbulent fluctuations in velocity and magnetic field (possibly triggered by MRI) can provide a mean electromotive force and amplify seed magnetic fields.

Here we are going to show how to move from classical MHD recipes to a form suitable for numerical GRMHD.

As a first example: *kinematic* dynamo in thick accretion tori.

Dynamo action in GRMHD

Previous works: kinematic dynamo in thick disks *neglecting the displacement current* (Khanna & Camenzind, 1996; Brandenburg, 1996).

Our ultimate goal is to perform fully dynamic GRMHD simulations of BH accretion from disks with dynamo action at work.
The steps so far have been:

- First covariant closure of the generalized Ohm's law for resistive GRMHD and dynamo action, adaptation to $3+1$, and implementation in the ECHO and X-ECHO codes:
  Bucciantini & Del Zanna, MNRAS 428, 71, 2013
- Introduction of high-order RK-IMEX schemes:
  Del Zanna, Bugli, Bucciantini, ASP Conf. Series 488, 217, 2014
- Study of the kinematic dynamo process in thick accretion disks around Kerr Black Holes:
  Bugli, Del Zanna, Bucciantini, MNRAS 440L, 41, 2014

Mean-field dynamo in classical MHD

Consider small-scale turbulent fluctuations in the fields $\boldsymbol{v}$ e $\boldsymbol{B}$:

$$\boldsymbol{v}(\boldsymbol{x},t) = \boldsymbol{v}_0(\boldsymbol{x},t) + \delta\boldsymbol{v}(\boldsymbol{x},t), \quad \boldsymbol{B}(\boldsymbol{x},t) = \boldsymbol{B}_0(\boldsymbol{x},t) + \delta\boldsymbol{B}(\boldsymbol{x},t)$$

[assumption of kinematical regime $\Rightarrow$ $\boldsymbol{v}_0(\boldsymbol{x},t)$ fixed].

The resistive induction equation for the mean magnetic field reads:

$$\partial_t \boldsymbol{B}_0 = \boldsymbol{\nabla} \times (\boldsymbol{v}_0 \times \boldsymbol{B}_0) + \eta_r \nabla^2 \boldsymbol{B}_0 + \boldsymbol{\nabla} \times \boldsymbol{\mathcal{E}}$$

$$\boldsymbol{\mathcal{E}} = \langle \delta\boldsymbol{v} \times \delta\boldsymbol{b} \rangle \simeq \alpha \boldsymbol{B}_0 - \beta \boldsymbol{\nabla} \times \boldsymbol{B}_0$$

$$\Downarrow$$

$$\partial_t \boldsymbol{B} = \boldsymbol{\nabla} \times (\boldsymbol{v} \times \boldsymbol{B}) + \eta \nabla^2 \boldsymbol{B} + \alpha \boldsymbol{\nabla} \times \boldsymbol{B}$$

- Increase of the magnetic resistivity ($\eta = \eta_r + \beta$)
- Generation of magnetic field parallel to the current ($\boldsymbol{J} = \boldsymbol{\nabla} \times \boldsymbol{B}$)
- Generalized Ohm's law ($\boldsymbol{E}' \equiv \boldsymbol{E} + \boldsymbol{v} \times \boldsymbol{B} = \eta \boldsymbol{J} - \alpha \boldsymbol{B}$)

The $\alpha - \Omega$ dynamo

Let us decompose the magnetic field (and the other quantities) as

$$\boldsymbol{B} = \boldsymbol{B}_P + B_T \boldsymbol{e}_T, \quad \boldsymbol{B}_P = \boldsymbol{\nabla} \times (A_T \boldsymbol{e}_T).$$

The induction equation is split as

$$\begin{aligned} \partial_t B_T + (\boldsymbol{U}_P \cdot \boldsymbol{\nabla}) B_T &= (\boldsymbol{B}_P \cdot \boldsymbol{\nabla}) U_T + \eta \nabla^2 B_T \\ \partial_t A_T + (\boldsymbol{U}_P \cdot \boldsymbol{\nabla}) A_T &= \alpha B_T + \eta \nabla^2 A_T \end{aligned}$$

- Differential rotation $\Rightarrow$ Generation of toroidal field (Ω effect)
- Toroidal field $\Rightarrow$ Generation of poloidal field (α effect)

$$\boldsymbol{B}_P \Rightarrow \boldsymbol{B}_T \Rightarrow \boldsymbol{B}_P \Rightarrow \ldots$$

Exponentially growing $\alpha - \Omega$ dynamo modes, damped by resistivity.

The solar cycle and the *butterfly diagram*

- Flux tubes of growing toroidal magnetic field emerge through the photosphere: formation of a Sun Spot
- Formation at latitudes $\pm 35°$
- Migration towards the equator
- Strong periodicity $\sim$ 11 yr (solar rotation < 1 month)

A possible mechanism at its basis is the $\alpha - \Omega$ dynamo.

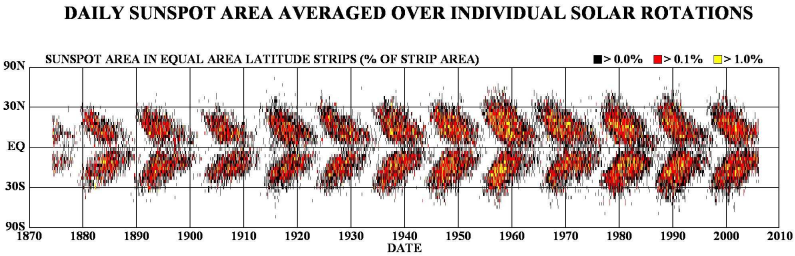

MRI and dynamo in stratified disks

Evolution of (classical) MHD turbulence in accretion disks is better studied in local shearing box simulations. Brief summary of results:

- MRI induces turbulence and the Shakura-Sunyaev term needed for angular momentum transport (Balbus & Hawley, 1991)
- Stratification allows for magnetic buoyancy (Brandenburg, 1995)
- Turbulent dynamo, butterfly diagrams, and sometimes (debated) magnetocentrifugally driven outflows (Davis et al., 2010; Flock et al., 2012; Bai & Stone, 2013; Fromang et al., 2013)

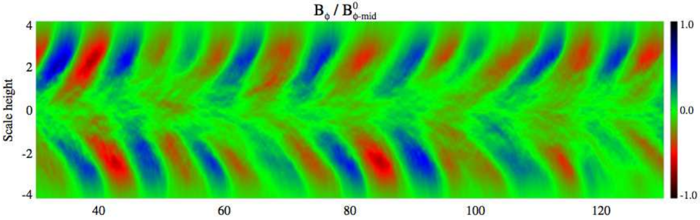

Non-ideal Ohm's law in $3+1$ GRMHD: formulation, methods, tests

The ECHO code for GRMHD

Numerical simulations will be performed with the *Eulerian Conservative High-Order* ECHO code (Del Zanna et al., 2007), a versatile tool for MHD and GRMHD combining shock-capturing properties and accuracy.

Main features (Londrillo & Del Zanna, 2000; 2004):

- conservative form, RK time-stepping,
- finite differences, high-order methods (CENO, WENO, MP...),
- simplified Riemann solvers: LLF, HLL, HLLC,
- F90, various geometries, different physical modules,
- Upwind Constrained Transport (UCT) based on 4-state B fluxes.

Upgrades:

- evolution of Einstein equations (Bucciantini & Del Zanna 2011),
- radiation hydrodynamics (Zanotti et al., 2011),
- resistivity and dynamo (Bucciantini & Del Zanna, 2013).

Conservative 3 + 1 equations

In numerical GRMHD the spacetime metric is split in the 3 + 1 form

$$\mathrm{d}s^2 = -\alpha^2 \mathrm{d}t^2 + \gamma_{ij}\,(\mathrm{d}x^i + \beta^i \mathrm{d}t)(\mathrm{d}x^j + \beta^j \mathrm{d}t),$$

where α and β^i are, respectively, the *lapse function* and *shift vector* ($\alpha = 1$, $\beta^i = 0$ in Newtonian MHD), and γ_{ij} is the 3-metric tensor.

The conservative equations in ECHO for *ideal* GRMHD are

$$\frac{\partial}{\partial t}\sqrt{\gamma}\begin{bmatrix} D \\ S_j \\ E \\ B^j \end{bmatrix} + \frac{\partial}{\partial x^i}\sqrt{\gamma}\begin{bmatrix} DV^i \\ \alpha S^i_j - \beta^i S_j \\ \alpha S^i - \beta^i E \\ V^i B^j - V^j B^i \end{bmatrix} = \sqrt{\gamma}\begin{bmatrix} 0 \\ \frac{1}{2}\alpha S^{ik}\partial_j \gamma_{ik} + S_i \partial_j \beta^i - E\partial_j \alpha \\ \alpha S^{ij} K_{ij} - S^j \partial_j \alpha \\ 0 \end{bmatrix}$$

where K_{ij} is the *extrinsic curvature* and $V^i = \alpha v^i - \beta^i$ is the *transport velocity*.

Let us now relax the ideal Ohm law (the same in MHD and GRMHD):

$$\boldsymbol{E} = -\boldsymbol{v} \times \boldsymbol{B}.$$

Covariant generalized Ohm's Law

Covariant Maxwell's equations:

$$\nabla_\mu F^{\mu\nu} = -I^\nu, \quad \nabla_\mu F^{*\mu\nu} = 0$$

$$F^{\mu\nu} = u^\mu e^\nu - u^\nu e^\mu + \epsilon^{\mu\nu\lambda\kappa} b_\lambda u_\kappa, \quad I^\mu = q_0 u^\mu + j^\mu$$

Fully covariant formulation for a resistive plasma with dynamo action:

$$\boxed{e^\mu = \eta j^\mu + \xi b^\mu}$$

$$(\xi \equiv -\alpha_{dyn}, \quad \eta = \eta_r + \beta_{dyn})$$

$$\Downarrow$$

$$\Gamma[\boldsymbol{E} + \boldsymbol{v} \times \boldsymbol{B} - (\boldsymbol{E} \cdot \boldsymbol{v})\boldsymbol{v}] = \eta(\boldsymbol{J} - q\boldsymbol{v}) + \xi\Gamma[\boldsymbol{B} - \boldsymbol{v} \times \boldsymbol{E} - (\boldsymbol{B} \cdot \boldsymbol{v})\boldsymbol{v}]$$

Classical limit ($|\boldsymbol{v}| \ll 1$, $|\boldsymbol{E}| \ll |\boldsymbol{B}|$):

$$\boldsymbol{E}' \equiv \boldsymbol{E} + \boldsymbol{v} \times \boldsymbol{B} = \eta \boldsymbol{J} + \xi \boldsymbol{B}$$

Implementation within 3 + 1 GRMHD

Maxwell's equations in 3 + 1 form are:

$$\gamma^{-1/2}\partial_t\left(\gamma^{1/2}\boldsymbol{B}\right) + \boldsymbol{\nabla}\times(+\alpha\boldsymbol{E} + \boldsymbol{\beta}\times\boldsymbol{B}) = 0, \qquad (\boldsymbol{\nabla}\cdot\boldsymbol{B} = 0)$$

$$\gamma^{-1/2}\partial_t\left(\gamma^{1/2}\boldsymbol{E}\right) + \boldsymbol{\nabla}\times(-\alpha\boldsymbol{B} + \boldsymbol{\beta}\times\boldsymbol{E}) = -(\alpha\boldsymbol{J} - q\boldsymbol{\beta}), \qquad (\boldsymbol{\nabla}\cdot\boldsymbol{E} = q)$$

Computing $\boldsymbol{J}$ from Ohm's law we get:

$$\gamma^{-1/2}\partial_t(\gamma^{1/2}\boldsymbol{E}) + \boldsymbol{\nabla}\times(-\alpha\boldsymbol{B} + \boldsymbol{\beta}\times\boldsymbol{E}) + (\alpha\boldsymbol{v} - \boldsymbol{\beta})\boldsymbol{\nabla}\cdot\boldsymbol{E} =$$
$$-\alpha\Gamma\,\eta^{-1}\{[\boldsymbol{E} + \boldsymbol{v}\times\boldsymbol{B} - (\boldsymbol{E}\cdot\boldsymbol{v})\boldsymbol{v}] - \xi[\boldsymbol{B} - \boldsymbol{v}\times\boldsymbol{E} - (\boldsymbol{B}\cdot\boldsymbol{v})\boldsymbol{v}]\}$$

A stiff equation: terms $\propto \eta^{-1}$ can evolve on time scales $\tau_\eta \ll \tau_h$.

Letting $\eta = \xi = 0$ we retrieve the ideal case:

$$\boldsymbol{E} + \boldsymbol{v}\times\boldsymbol{B} - (\boldsymbol{E}\cdot\boldsymbol{v})\boldsymbol{v} = 0 \Rightarrow \boldsymbol{E} = -\boldsymbol{v}\times\boldsymbol{B}.$$

Stiff relaxation equations

System of hyperbolic ODEs + stiff relaxation equations:

$$\begin{aligned} \boldsymbol{X} = \gamma^{1/2}\boldsymbol{E}: \quad \partial_t \boldsymbol{X} &= \boldsymbol{Q}_X(\boldsymbol{X},\boldsymbol{Y}) + \boldsymbol{R}_X(\boldsymbol{X},\boldsymbol{Y}) \\ \boldsymbol{Y} = \gamma^{1/2}\boldsymbol{B}: \quad \partial_t \boldsymbol{Y} &= \boldsymbol{Q}_Y(\boldsymbol{X},\boldsymbol{Y}) \end{aligned}$$

- $\boldsymbol{Q}_{X,Y}$= non stiff terms, evolving as $\sim \tau_h$
- $\boldsymbol{R}_X$= stiff terms $\propto \eta^{-1}$, evolving as $\sim \tau_\eta \ll \tau_h$

We need appropriate techniques to evolve the system, even for $\xi = 0$:

- Splitting methods
  (Komissarov, 2007; Takamoto & Inoue, 2011; Takahashi et al., 2013).
- Discontinuous Galerkin methods
  (Dumbser & Zanotti, 2009; Zanotti & Dumbser, 2011).
- Implicit-Explicit RK methods
  (Palenzuela et al., 2009; Bucciantini & Del Zanna, 2013; Palenzuela, 2013; Dionysopoulou et al., 2013; Del Zanna et al. / Bugli et al., 2014).

High-order IMEX schemes

High-order time integration via IMEX Runge-Kutta methods with Strong Stability Preserving properties (Pareschi & Russo, 2005):

- Phase 1: Explicit integration

$$\begin{aligned} \boldsymbol{X}_*^{(i)} &= \boldsymbol{X}^n + \Delta t \textstyle\sum_{j=1}^{i-1} \tilde{a}_{ij} \boldsymbol{Q}_X[\boldsymbol{X}^{(j)}, \boldsymbol{Y}^{(j)}] + \Delta t \textstyle\sum_{j=1}^{i-1} a_{ij} \boldsymbol{R}_X[\boldsymbol{X}^{(j)}, \boldsymbol{Y}^{(j)}] \\ \boldsymbol{Y}_*^{(i)} &= \boldsymbol{Y}^n + \Delta t \textstyle\sum_{j=1}^{i-1} \tilde{a}_{ij} \boldsymbol{Q}_Y[\boldsymbol{X}^{(j)}, \boldsymbol{Y}^{(j)}] \end{aligned}$$

- Phase 2: Implicit integration

$$\begin{aligned} \boldsymbol{X}^{(i)} &= \boldsymbol{X}_*^{(i)} + a_{ii} \Delta t \boldsymbol{R}_X[\boldsymbol{X}^{(i)}, \boldsymbol{Y}_*^{(i)}] \\ \boldsymbol{Y}^{(i)} &= \boldsymbol{Y}_*^{(i)} \end{aligned}$$

- Phase 3: Final step

$$\begin{aligned} \boldsymbol{X}^{n+1} &= \boldsymbol{X}^n + \Delta t \textstyle\sum_{i=1}^{\nu} \tilde{\omega}_i \boldsymbol{Q}_X[\boldsymbol{X}^{(i)}, \boldsymbol{Y}^{(i)}] + \Delta t \textstyle\sum_{i=1}^{\nu} \omega_i \boldsymbol{R}_X[\boldsymbol{X}^{(i)}, \boldsymbol{Y}^{(i)}] \\ \boldsymbol{Y}^{n+1} &= \boldsymbol{Y}^n + \Delta t \textstyle\sum_{i=1}^{\nu} \tilde{\omega}_i \boldsymbol{Q}_Y[\boldsymbol{X}^{(i)}, \boldsymbol{Y}^{(i)}] \end{aligned}$$

Numerical tests: 1D current sheet

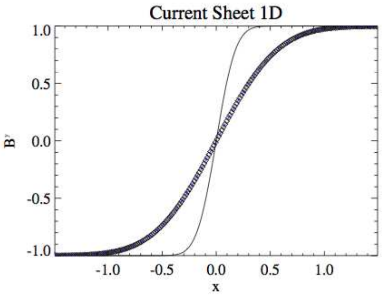

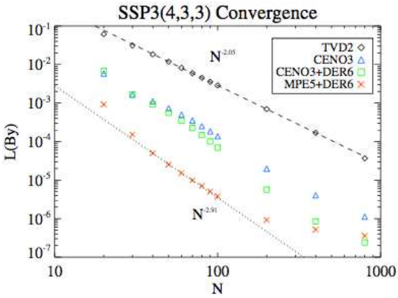

Diffusion equation:

$$p \gg B^2 \Rightarrow B^y(x,t) = B_0 \mathrm{erf}\left(\frac{x}{2\sqrt{\eta t}}\right); \quad [\eta = 0.01, t = 1, 10]$$

Numerical tests: 1D dynamo

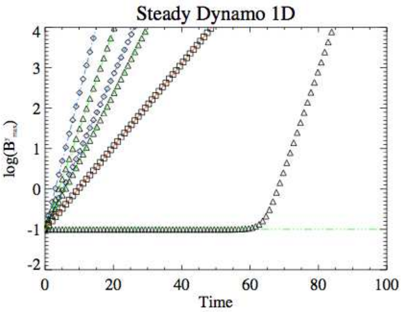

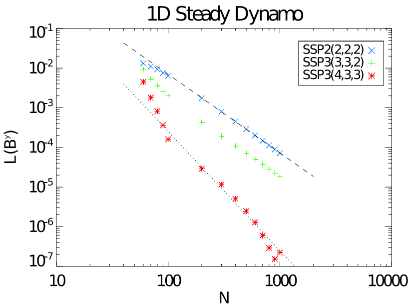

Exponentially growing dynamo modes:

$$B^y(x,t) = B_0 \exp(\gamma t)\cos(kx), \quad \gamma = \frac{\sqrt{1+4\eta k(\xi - \eta k)} - 1}{2\eta}$$

Kinematic dynamo in accretion tori

GRHD thick torus

Equilibrium: axisymmetric torus in Kerr metric and Boyer-Lindquist coordinates (Abramowicz et al., 1978; Font & Daigne, 2002).

Bernoulli equation for barotropic EOS $p \propto (\rho h)^\kappa$, differential rotation $\Omega = u^\phi / u_t$, constant specific angular momentum $l_0 = -u_\phi / u_t$:

$$W - W_{\rm in} + \frac{\kappa}{\kappa - 1} \frac{p}{\rho h} = 0, \quad W = \ln |u_t| = \frac{1}{2} \ln \left(\frac{g_{t\phi}^2 - g_{rr} g_{\phi\phi}}{g_{\phi\phi} + 2 g_{t\phi} l_0 + g_{tt} l_0^2} \right)$$

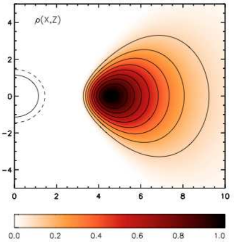

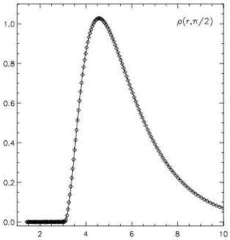

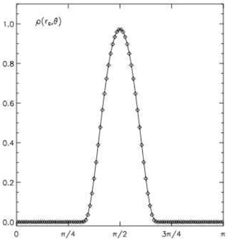

Numerical set up

- Spatial interpolation: MPE5 + DER6.
- Time integration: IMEX-RK SSP3(4,3,3).
- Two-dimensional grid in (r, θ).
- Maximally rotating Kerr BH ($a = 0.99$).
- Ideal, corotating atmosphere.
- Spatially varying ξ and η.
- Different choices of dynamo numbers:

$$C_\xi = \frac{\xi R}{\eta} \geq 1, \qquad C_\Omega = \frac{\Delta\Omega R^2}{\eta} \gg 1$$

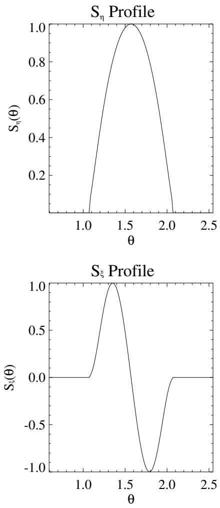

Initial seed magnetic field

- Initial seed magnetic field $B \sim 10^{-6}$ either toroidal or poloidal.
- Initial ideal electric field ($\boldsymbol{E} = -\boldsymbol{v} \times \boldsymbol{B}$).

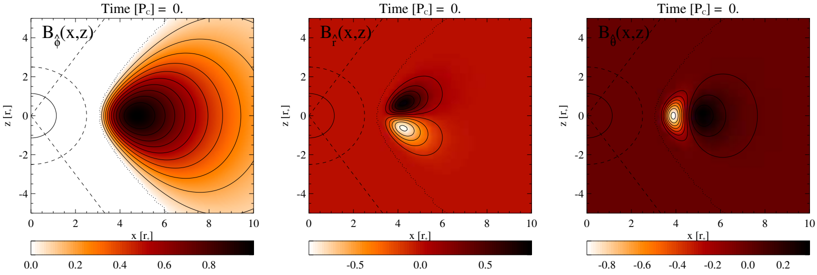

Study of the Ω effect vs resistivity

- No dynamo action ($\xi = 0$).
- Competition between ideal Ω effect and resistive η dissipation.
- Estimate of saturation toroidal field:

$$\Delta B \sim T \Delta\Omega |\boldsymbol{B}_P| \sim -T \frac{\eta}{R^2} B \Rightarrow$$

$$B_{sat} \sim \frac{\Delta\Omega R^2}{\eta} |\boldsymbol{B}_P| \equiv C_\Omega |\boldsymbol{B}_P|$$

- Long-term runs ($P_c = 76.5$) confirm this ($\eta = 0, 10^{-5}, 10^{-4}, 10^{-3}, 10^{-2}$).

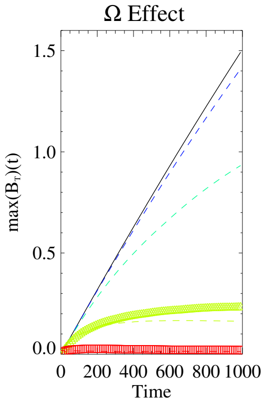

Evolution of the toroidal component

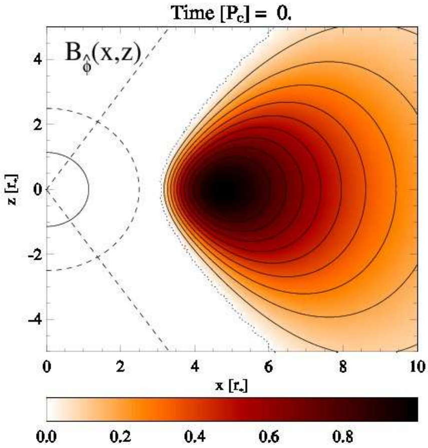

Evolution of the poloidal components

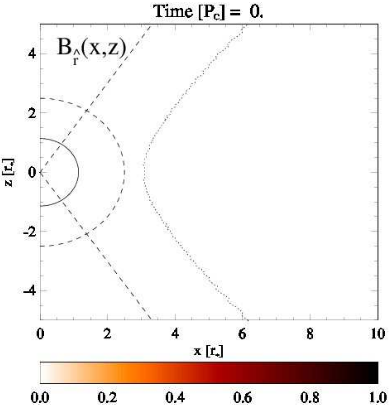

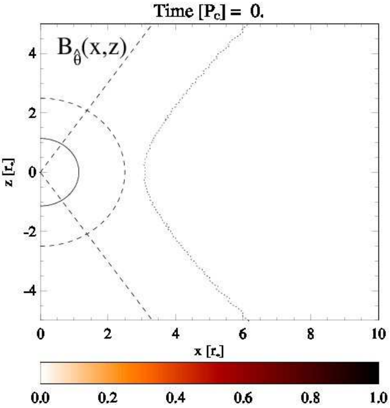

Growth rate and ratio B_P / B_T

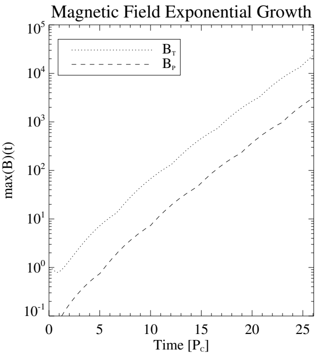

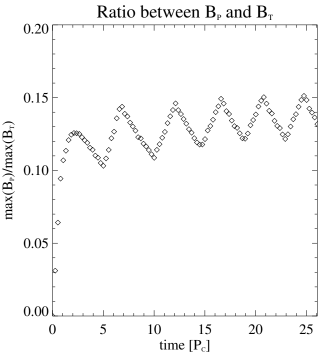

Butterfly diagram

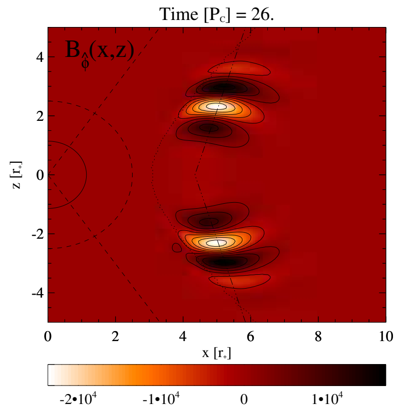

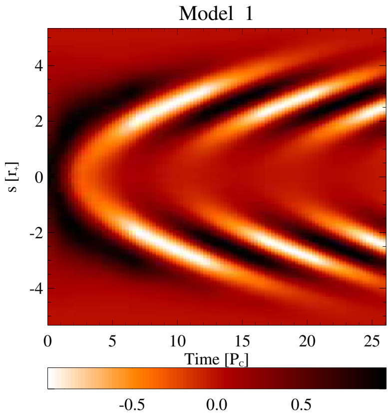

Migration reversal

The *solar analogy* is reproduced by choosing $\xi < 0 \Rightarrow \alpha_{dyn} > 0$:

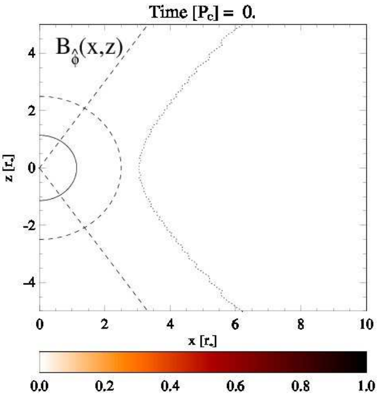

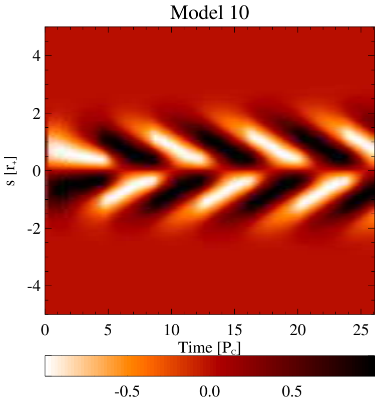

Summary of results

	$\boldsymbol{B}_{\rm init}$	C_ξ	C_Ω	Growth Rate	Period	s_{max}	$(B_P)_{max}/(B_T)_{max}$
Model 1	$\boldsymbol{B}_T$	5	400	0.30	10.34	2.90	0.12
Model 2	$\boldsymbol{B}_T$	-5	400	0.25	9.14	0.67	0.12
Model 3	$\boldsymbol{B}_T$	25	400	1.26	3.31	2.42	0.36
Model 4	$\boldsymbol{B}_T$	1	400	0.06	33.14	3.18	0.04
Model 5	$\boldsymbol{B}_T$	5	80	0.37	6.63	3.11	0.17
Model 6	$\boldsymbol{B}_T$	5	2000	0.21	17.23	2.64	0.07
Model 7	$\boldsymbol{B}_P$	5	400	0.30	10.34	2.95	0.12
Model 8	$\boldsymbol{B}_P$	25	400	1.26	3.31	2.36	0.36
Model 9	$\boldsymbol{B}_P$	1	400	0.06	34.47	3.13	0.04
Model 10	$\boldsymbol{B}_P$	-5	400	0.25	9.54	0.82	0.12

Conclusions and future work

Conclusions

Summary of main results:

- resistivity and dynamo action in ECHO and X-ECHO with high-order IMEX schemes,
- first resistive GRMHD simulation of dynamo action in thick disks,
- exponential growth of toroidal and poloidal magnetic fields,
- timescale depends on microphysics, not on rotation period,
- migration of the fields towards/from the equator, in strong analogy with the Sun and with shearing box simulations.

Possible developments and applications:

- improvement in the model assumptions: dynamical regime and accretion, feedback (quenching) on η and ξ, different M and a,
- possible connections with phenomena with unexplained time periodicity scales: variable accretion? Periodic BZ activations?

Future work

Beyond dynamo:

- A general ECHO code for relativistic dissipative plasmas in $3+1$ GRMHD (resistivity, viscosity, heat conduction).
- High-order IMEX schemes for all stiff dissipative equations.
- Unification with the version for radiation RHD (Zanotti et al., 2011; Roedig et al., 2012).

Achievements so far:

- ECHO-QGP: viscous RHD for the Quark-Gluon Plasma in heavy-ion collisions (Del Zanna et al., 2013).
- Second-order Israel-Stewart theory applied (with relaxation equations).

ECHO-QGP: viscous RHD for heavy-ion collisions

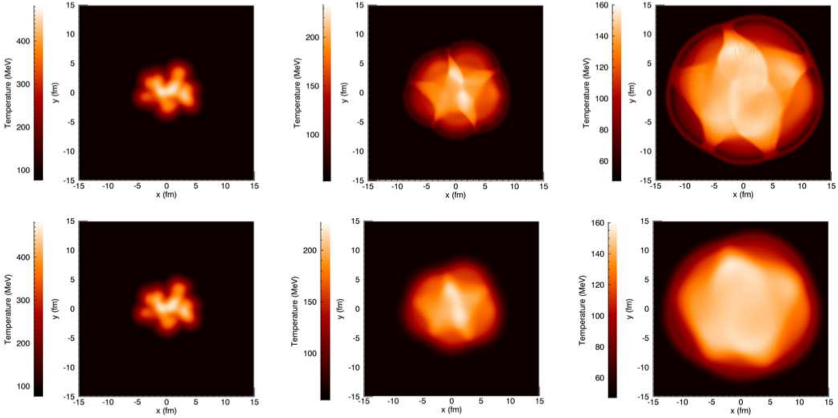

Thank you!